DOI 10.1007/s10946-021-09956-3
Journal of Russian Laser Research, Volume 42, Number 2, March, 2021

A NEW ADE-TLM FOR LORENTZ DISPERSIVE MEDIUM

Abdellah Attalhaoui,[1*] Hamid Bezzout,[2] Mohamed Habibi,[1] and Hanan El Faylali[2]

[1] *The Laboratory of Electrical Engineering and Energy Systems*
Ibn Tofail University
Kenitra, Morocco

[2] *The Laboratory of Informatics, Systems and Optimization*
Ibn Tofail University,
Kenitra, Morocco

*Corresponding author e-mail: abdellah.attalhaoui@gmail.com

Abstract

We present a new numerical algorithm for the simulation of dispersive media. This model named ADE-TLM is based on the transmission line modeling method with the symmetrical condensed node (SCN-TLM) and novel voltage sources and exploits the polarization current density J along with the voltage electric as well as the average approximation. We extend the proposed algorithm to media with dispersions described by multiple second-order Lorentz poles; the obtained results of the reflection and transmission coefficients are compared with analytical solutions.

Keywords: Lorentz media, ADE-TLM, SCN-TLM, current density.

1. Introduction

Since the introduction of the symmetrical condensed node (SCN) for the numerical solution of the Maxwell equations in 1987 by Johns [1], the transmission line modeling (TLM) method has been widely used to treat the problems of the electromagnetic wave propagations in dispersive media. This time-domain method makes the analogy between the electromagnetic field components and the electrical quantities. Several TLM-based algorithms for the analysis of dispersive media have been reported in the literature. One approach is including the Z-transform technique [2], which was applied to linear frequency-dependent isotropic materials and extended to anisotropic materials. Other approaches include the constant recursive convolution (CRC) technique [3], and its improved CDRC-TLM [4] and PLCDRC-TLM [5], which are applied to magnetized plasma. The other approach includes JE-TLM [6], which is applied to isotropic plasma by exploiting the dependence of the current density J and the electric field E.

The auxiliary differential equation (ADE-TLM) has been used to model linear dispersive media exploiting the relationship between polarization and the electric field [7] and to model dispersive chiral media [8] by exploiting electric and magnetic current densities. The ADE method has the advantage that it is attractive for modeling nonlinear dispersive media. Compared to RC and PLRC schemes, which have been exploited in [9, 10], the ADE scheme requires the same or less memory [11]. However, we use aforementioned ADE-TLM algorithm based on the SCN-TLM with 12 principal ports to model the free space and 3 additional ports used as voltage sources to model the properties of Lorentz media, i.e., to model Lorentz dispersive media by applying the ADE to the polarization current density, not to the polarization density. We confirm this approach by comparing the reflection and transmission coefficients with analytical solutions, which are compared with simulation that involves single-pole dispersion in [9, 12] and the cases involving a multi-term dispersion in [10, 13, 14].

Manuscript submitted by the authors in English on October 8, 2020.

2. ADE-TLM Method and Formulation

For the second-order Lorentz medium, the Maxwell equations related to the polarization current density are given as follows:

$$\nabla \times \mathbf{E} = -\mu_0 \frac{\partial \mathbf{H}}{\partial t}\,, \tag{1}$$

$$\nabla \times \mathbf{H} = \varepsilon_0 \varepsilon_\infty \frac{\partial \mathbf{E}}{\partial t} + \mathbf{J}\,, \tag{2}$$

where $\mathbf{E}$ and $\mathbf{H}$ are the electric and magnetic field strengths, $\mathbf{J} = \sum\limits_{p=1}^{p} \mathbf{J}_p$ is the polarization current density, ε_0 is permittivity of vacuum, and μ_0 is magnetic permeability of vacuum. The relative permittivity of the Lorentz medium with multi-term dispersion can be described as [15]

$$\varepsilon(\omega) = \varepsilon_\infty + (\varepsilon_s - \varepsilon_\infty) \sum_{p=1}^{p} \frac{G_p w_p^2}{w_p^2 + 2jw\delta_p - w^2}\,, \tag{3}$$

where ε_∞ is the static permittivity, ω_p is the pth Lorentz characteristic resonant frequency, and δ_p is the pth damping factor, with the condition that $\sum\limits_{p=1}^{p} G_p = 1$.

A polarization current density due to a single pole in the frequency domain reads [11]

$$\tilde{\mathbf{J}}_p = (\varepsilon_s - \varepsilon_\infty)\, w_p^2 \varepsilon_0 G_p \left(\frac{jw}{w_p^2 + 2jw\delta_p - w^2} \right) \tilde{\mathbf{E}}\,. \tag{4}$$

Multiplying both sides of Eq. (4) by $(w_p^2 + 2jw\delta_p - w^2)$ and transforming to the time domain, we arrive at

$$w_p^2 \mathbf{J}_p + 2\delta_L \frac{\partial \mathbf{J}_p}{\partial t} + \frac{\partial^2}{\mathbf{J}_p} \partial t^2 = (\varepsilon_s - \varepsilon_\infty) w_p^2 \varepsilon_0 G_p \frac{\partial \mathbf{E}}{\partial t}\,. \tag{5}$$

Applying the finite difference time to Eq. (5), the linear polarization current density centered at step $n+1$ can be expressed as follows:

$$\mathbf{J}_p^{n+1} = \alpha_p \mathbf{J}_p^n + \xi_p \mathbf{J}_p^{n-1} + \gamma_p \frac{\mathbf{E}^{n+1} - \mathbf{E}^{n-1}}{2\Delta t}\,, \tag{6}$$

where

$$\alpha_p = \frac{2 - w_L^2 (\Delta t)^2}{1 + \delta_L \Delta t}, \qquad \xi_p = \frac{\delta_L \Delta t - 1}{1 + \delta_L \Delta t}, \qquad \gamma_p = \frac{G_p \varepsilon_0 (\varepsilon_s - \varepsilon_\infty) w_L^2 (\Delta t)^2}{1 + \delta_L \Delta t}\,. \tag{7}$$

The temporal discretization of Eq. (2) centered at step $n + 1/2$ provides

$$\mathbf{E}^{n+1} = \mathbf{E}^n + \frac{\Delta t}{\varepsilon_0} (\nabla \times \mathbf{H}^{n+1/2} - \mathbf{J}^{n+1/2}). \tag{8}$$

The polarization current centered at step $n + 1/2$ can be obtained from Eq. (6) by

$$\mathbf{J}^{n+1/2} = \frac{1}{2} (\mathbf{J}^{n+1} + \mathbf{J}^n)\,. \tag{9}$$

For a uniform mesh, the TLM method transforms the electric field to voltage, using this equivalence

$$\mathbf{E}^n = \frac{\mathbf{V}^n}{\Delta l}\,. \tag{10}$$

In view of Eq. (10), Eq. (6) and Eq. (8) can be rewritten, respectively, as follows:

$$\mathbf{J}_p^{n+1} = \alpha_p \mathbf{J}_p^n + \xi_p \mathbf{J}_p^{n-1} + \gamma_p \frac{\mathbf{V}^{n+1} - \mathbf{V}^{n-1}}{2\Delta l \Delta t}\,, \tag{11}$$

$$\mathbf{V}^{n+1} = \mathbf{V}^n + \frac{\Delta l \Delta t}{\varepsilon_0}\left(\nabla \times \mathbf{H}^{n+1/2} - \mathbf{J}^{n+1/2}\right). \tag{12}$$

To make ADE-TLM more efficient, we need to update Eq. (11), using the average approximation described in [16]; we obtain

$$\mathbf{V}^n = \frac{\mathbf{V}^{n+1} + \mathbf{V}^{n-1}}{2}\,. \tag{13}$$

Substituting Eq. (13) into Eq. (11), we arrive at

$$\mathbf{J}_p^{n+1} = \alpha_p \mathbf{J}_p^n + \xi_p \mathbf{J}_p^{n-1} + \gamma_p \frac{\mathbf{V}^n - \mathbf{V}^{n-1}}{\Delta l \Delta t}\,. \tag{14}$$

Applying the SCN-TLM model [17] to Eq. (1), we find

$$\begin{pmatrix} \nabla \times H_x^{n+1/2} \\ \nabla \times H_y^{n+1/2} \\ \nabla \times H_z^{n+1/2} \end{pmatrix} = \begin{pmatrix} \frac{\varepsilon_0}{2\,\Delta t\,\Delta l}\left[(V_1^i + V_2^i + V_9^i + V_{12}^i)^{n+1} - (V_1^r + V_2^r + V_9^r + V_{12}^r)^n\right] \\ \frac{\varepsilon_0}{2\,\Delta t\,\Delta l}\left[(V_3^i + V_4^i + V_8^i + V_{11}^i)^{n+1} - (V_3^r + V_4^r + V_8^r + V_{11}^r)^n\right] \\ \frac{\varepsilon_0}{2\,\Delta t\,\Delta l}\left[(V_5^i + V_6^i + V_7^i + V_{10}^i)^{n+1} - (V_5^r + V_6^r + V_7^r + V_{10}^r)^n\right] \end{pmatrix}. \tag{15}$$

Here,

$$\begin{pmatrix} V_1^r + V_2^r + V_9^r + V_{12}^r \\ V_3^r + V_4^r + V_8^r + V_{11}^r \\ V_5^r + V_6^r + V_7^r + V_{10}^r \end{pmatrix}^n = \begin{pmatrix} V_1^i + V_2^i + V_9^i + V_{12}^i \\ V_3^i + V_4^i + V_8^i + V_{11}^i \\ V_5^i + V_6^i + V_7^i + V_{10}^i \end{pmatrix}^n + \begin{pmatrix} V_{sx} \\ V_{sy} \\ V_{sz} \end{pmatrix}^n. \tag{16}$$

Substituting Eq. (15) into Eq. (12), exploiting Eq. (16), and using the symmetrical condensed node (SCN-TLM), we express the total electric as follows:

$$\begin{pmatrix} V_x^{n+1} \\ V_y^{n+1} \\ V_z^{n+1} \end{pmatrix} = \begin{pmatrix} \frac{2}{4 + Y_{ox}} \\ \frac{2}{4 + Y_{oy}} \\ \frac{2}{4 + Y_{oz}} \end{pmatrix} \begin{pmatrix} \left[V_1^i + V_2^i + V_9^i + V_{12}^i + 1/2\; V_{sx}\right]^{n+1} \\ \left[V_3^i + V_4^i + V_8^i + V_{11}^i + 1/2\; V_{sy}\right]^{n+1} \\ \left[V_5^i + V_6^i + V_7^i + V_{10}^i + 1/2\; V_{sz}\right]^{n+1} \end{pmatrix}. \tag{17}$$

The normalized admittances Y_{ox}, Y_{oy}, and Y_{oz} read

$$Y_{ou} = 4(\varepsilon_\infty - 1). \tag{18}$$

The voltage sources V_{sx}, V_{sy}, and V_{sz} are

$$V_{su}^{n+1} = -V_{su}^{n} - \frac{\Delta l \Delta t}{2\,\varepsilon_0} \sum_{p=1}^{p} (J_{pu}^{n+1} + J_{pu}^{n}), \tag{19}$$

where $u \in \{x, y, z\}$.

The complete procedure of ADE-TLM in the second-order Lorentz medium goes like this:

Starting with stored values of V^{n-1}, V^n, J_p^n, and J_p^{n-1}.

We first update J_p^{n+1} made by Eq. (14), then the obtained values of J_p^{n+1} are inserted in the voltage sources using Eq. (19).

The V^{n+1} described in Eq. (17) is updated from normalized admittance and voltage sources in view of Eqs. (18) and (19), respectively.

Finally, the stored values of V^{n+1} is used to simulate the reflected pulses, employing the scattering matrix, and to simulate the propagation to adjacent node, employing the connexion matrix.

3. Numerical Result

In order to demonstrate the accuracy of the ADE-TLM approach, we consider three examples, calculate the reflection and transmission coefficients, and compare to analytical solutions. For all cases, a plane Gaussian wave is normally incident from air onto a dispersive Lorentz medium. First, for a dispersive medium described with a single second-order Lorentz pole, the network is divided into $(1, 1, 1000)\Delta l$, with the spatial thickness $\Delta l = 250$ μm. The one second-order Lorentz pole occupies cells from 50 to 1000, and the constants determining the complex permittivity for the medium are given as $w_0 = 2\pi \cdot 20 \cdot 10^9$ rad/s, $\varepsilon_s = 3.0$, $\varepsilon_\infty = 1.5$, and $\delta_{\text{Lorentz}} = 0.1\ w_0$. The reflection coefficient of air Lorentz is simulated, using the fast Fourier transform (FFT) of the time history of the reflected pulse and the FFT of the time history of the incident pulse at the interface (at cell $49\Delta l$).

We calculate the analytical solution of the reflection coefficient, using the following expression:

$$|\Gamma(\omega)| = \left| \frac{\sqrt{\varepsilon_0} - \sqrt{\varepsilon^*(\omega)}}{\sqrt{\varepsilon_0} + \sqrt{\varepsilon^*(\omega)}} \right|, \tag{20}$$

where $\varepsilon^*(\omega)$ is the complex permittivity.

As shown in Fig. 1, the result of simulation of the reflection coefficient at the interface, using the ADE-TLM algorithm and analytical solution, agree very well [9, 10].

Second, for a dispersive medium described with two second-order Lorentz poles, the network is divided into $(1, 1, 1500)\Delta l$, with the spatial thickness $\Delta l = 37.5$ μm; the left 500 lattices are for the air, and other 1000 lattices are occupied by Lorentz medium. The constants determining the complex permittivity for the medium are $\varepsilon_s = 3.0$, $\varepsilon_\infty = 1.5$, $w_1 = 2\pi \cdot 20 \cdot 10^9$ rad/s, $\delta_1 = 0.1\ w_1$, $w_2 = 2\pi \cdot 50 \cdot 10^9$ rad/s, $\delta_2 = 0.1\ w_2$, $G_1 = 0.4$, and $G_2 = 0.6$. The reflection air – Lorentz coefficient is simulated, using the FFT of the time history of the reflected pulse and the FFT of the time history of the incident pulse at the interface (at cell $499\Delta l$).

In Fig. 2, we show the simulation result of the reflection coefficient at the interface; one can see that the result of ADE-TLM and analytical solution given by Eq. (20) agree very well [10, 13].

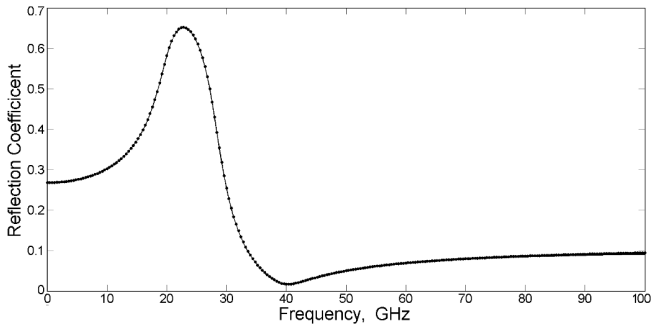

Fig. 1. Comparison of the reflection coefficient for the single Lorentzian dispersion case by the algorithm proposed (the solid curve) and the analytical solution (points).

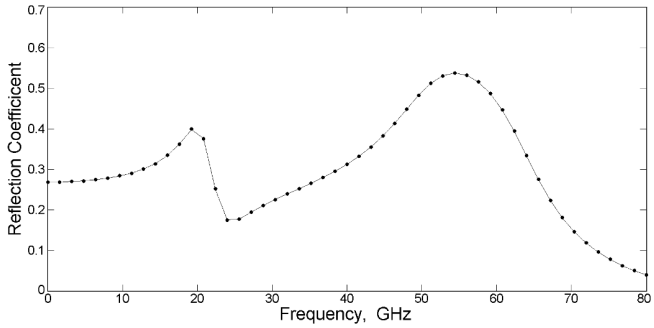

Fig. 2. Comparison of the reflection coefficient for multipole dispersion case by the algorithm proposed (the solid curve) and the analytical solution (points).

Finally, for a dispersive medium described with Lorentz slab, the network is divided into $(1, 1, 800)\Delta l$, with the spatial step $\Delta l = 75.0$ μm, and the Lorentz slab occupying cells 300 through 500 and keeping two second-order Lorentz poles, the same last constants which determine the complex permittivity.

We simulated the reflection coefficient of Lorentz slab using the FFT of the time history of the reflected pulse and the FFT of the time history of the incident pulse at the interface (at cell $299\Delta l$). We simulated the transmission coefficient of Lorentz slab, using the FFT of the time history of the transmitted pulse and the FFT of the time history of the incident pulse behind the Lorentz slab (at cell $501\Delta l$). We calculated the analytical solutions of reflection and transmission coefficients using the following expressions [15]:

$$\Gamma = \frac{\Gamma_{12} + \Gamma_{23} e^{-j2\beta_p d}}{1 + \Gamma_{12}\Gamma_{23} e^{-j2\beta_p d}}, \qquad T = \frac{T_{12} T_{23} e^{-j\beta_p d}}{1 + \Gamma_{12}\Gamma_{23} e^{-j2\beta_p d}}, \tag{21}$$

where d is the thickness of the Lorentz media, and β_p is the phase constant in the Lorentz media.

In Fig. 3, we show that the ADE-TLM results and the analytical solution for Lorentz slab are in excellent agreement [14].

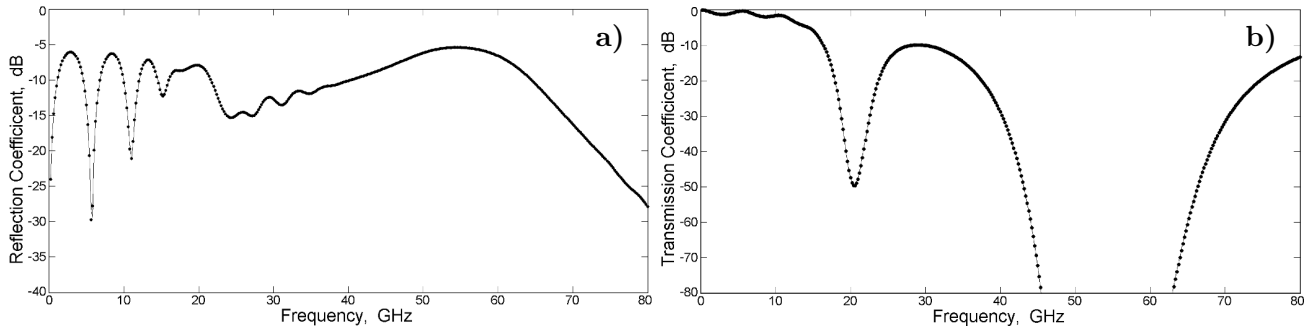

Fig. 3. Comparison of the reflection (a) and transmission (b) coefficients for the Lorentz-slab case by the algorithm proposed (the solid curve) and analytical solutions (points).

4. Summary

In this paper, we developed a novel transmission line modeling (TLM) for the second-order Lorentz dispersive medium, called the ADE-TLM. This approach exploits the relationship between the polarization current density, the voltage electric, and the average approximation. In this model, we introduced voltage sources modeling linear properties and normalized admittance concept. For extension to multi-term dispersion by a simple addition of the current density terms related to electric field, the ADE-TLM appears simpler to implement, and its accuracy is verified by calculating the reflection and transmission coefficients. Compared to RC and PLRC schemes, the ADE scheme needs the same or less number of unknowns to be stored.

References

1. P. B. Johns, *IEEE Trans. Microwave Theor. Tech.*, **35**, 370 (1987).
2. J. Paul, C. Christopoulos, and D. W. P. Thomas, *IEEE Trans. Antennas Propag.*, **47**, 1528 (1999).
3. M. Iben Yaich, M. Khalladi, I. Zekik, and J. A. Morente, *IEEE Microw. Wireless Compon. Lett.*, **12**, 293 (2002).
4. S. El Adraoui, M. Khalid, A. Zugari, et al., *Optik*, **125**, 276 (2014).
5. K. Mounirh, S. El Adraoui, M. Charif, et al., *Optik*, **126**, 1479 (2015).
6. R. Abrini, M. Iben Yaich, and M. Khalladi, *IEICE Electron. Express*, **4**, 492 (2007).
7. H. El Faylali, M. Iben Yaich, and M. Khalladi, *Int. J. Emerg. Trends Electric, Electron.*, **5**, 119 (2013).
8. K. Mounirh, S. El Adraoui, Y. Ekdiha, et al.. *Prog. Electromag. Res.*, **64**, 157 (2018).
9. D. F. Kelley and R. J. Luebbers, *IEEE Trans. Antennas Propag.*, **44**, 792 (1996).
10. M. Khalladi and M. Iben Yaich, *IEICE Electron. Express*, **2**, 373 (2005).
11. A. Taflove and S. C. Hagness, *Computational Electrodynamics: The Finite-Difference Time-Domain Method*, 3rd ed., Artech House, Norwood, UK, (2005).
12. J. Paul, C. Christopoulos, and D. W. P. Thomas, *IEEE Trans. Antennas Propag.*, **47**, 1528 (1999).
13. R. J. Luebbers and F. Hunsberger, *IEEE Trans. Antennas Propag.*, **40**, 1297 (1992).
14. H. W. Yang, *Optik*, **124**, 1199 (2013).
15. C. A. Balanis, *Advanced Engineering Electromagnetics*, Wiley, New York (1989).
16. H. Jin and R. Vahldieck, *IEEE Trans. Microw. Theor. Tech.*, **42**, 2554 (1994).
17. C. Christopoulos, *The Transmission-Line Modeling Method (TLM)*, IEEE Series on Electromagnetic Wave Theory, New York (1995).